Cyanide Binding and Heme Cavity Conformational Transitions in *Drosophila melanogaster* Hexacoordinate Hemoglobin[†,‡]

Daniele de Sanctis,[§] Paolo Ascenzi,[||] Alessio Bocedi,[||] Sylvia Dewilde,[⊥] Thorsten Burmester,[@] Thomas Hankeln,[#] Luc Moens,[⊥] and Martino Bolognesi*[,+]

Instituto de Tecnologia Quimica e Biologica, Universidade Nova de Lisboa, P.O. Box 127, 2781-901 Oeiras, Portugal, National Institute for Infectious Diseases, IRCCS 'Lazzaro Spallanzani', Via Portuense 292, 00149 Roma, Italy, Department of Biomedical Sciences, University of Antwerp, Campus Drie Eiken, B-2610 Antwerp, Belgium, Institute of Zoology, Johannes Gutenberg University of Mainz, Müllerweg 6, D-55099 Mainz, Germany, Institute of Molecular Genetics, Johannes Gutenberg University of Mainz, Becherweg 32, D-55099 Mainz, Germany, and Department of Biomolecular Sciences and Biotechnology and CNR-INFM, University of Milano, Via Celoria 26, 20131 Milano, Italy

Received March 8, 2006; Revised Manuscript Received June 14, 2006

ABSTRACT: The reason for the presence of hemoglobin-like molecules in insects, such as *Drosophila melanogaster*, that live in fully aerobic environments has yet to be determined. Heme endogenous hexacoordination (where HisE7 and HisF8 axial ligands to the heme Fe atom are both provided by the protein) is a recently discovered mechanism proposed to modulate O_2 affinity in hemoglobins from different species. Previous results have shown that *D. melanogaster* hemoglobin 1 (product of the *glob1* gene) displays heme endogenous hexacoordination in both the ferrous and ferric states. Here we present kinetic data characterizing the exogenous cyanide ligand binding process, and the three-dimensional structure (at 1.4 Å resolution) of the ensuing cyano-met *D. melanogaster* hemoglobin. Comparison with the crystal structure of the endogenously hexacoordinated *D. melanogaster* hemoglobin shows that the transition to the cyano-met form is supported by conformational readjustment in the CD−D−E region of the protein, which removes HisE7 from the heme. The structural and functional features of *D. melanogaster* hemoglobin are examined in light of previous results achieved for human and mouse neuroglobins and for human cytoglobin, which display heme endogenous hexacoordination. The study shows that, despite the rather constant value for cyanide association rate constants for the ferric hemoproteins, different distal site conformational readjustments and/or heme sliding mechanisms are displayed by the known hexacoordinate hemoglobins as a result of exogenous ligand binding.

Insects inhale oxygen and exhale carbon dioxide by means of a tracheal system that connects their inner organs to the air, thus supporting passive diffusion of oxygen to the metabolically active tissues. Therefore, the occurrence of specific oxygen carriers was assumed to be unnecessary in this taxon (*1*, *2*). In contrast to this assumption, the occurrence of oxygen carriers has been reported in insects. Hemoglobins (Hbs)[1] have long been known to be present, at high concentrations, in the hemolymph or in specialized tissues of a few insect species that live in a temporarily hypoxic environment, such as the aquatic larvae of the chironimid midges, some aquatic Hemiptera, or larvae of the horse botfly *Gasterophilus intestinalis* (*3*). These Hbs have been thoroughly characterized at both the protein and gene levels (*4*−*8*). The presence of a hemocyanin was demonstrated in a stonefly, *Perla marginata* (Plecoptera), suggesting that certain basal insects have retained an ancestral blood-based mechanism of gas exchange and that respiration in insects is much more complex than expected (*9*).

Hbs present at low concentrations have been found in many bacteria, unicellular eukaryotes, and plants as well as in vertebrate and invertebrate tissues (*10*, *11*). Many of them, including the vertebrate neuroglobin and cytoglobin, display a hexacoordinated heme iron atom showing a His−Fe^{2+}−His structure (*12*−*14*). In these Hbs, an exogenous heme ligand (e.g., O_2) has to compete with the endogenous ligand

[†] This work was supported by an Italian Ministry of University FIRB grant to M.B., by EU Project "Neuroglobin and the survival of the neuron" to M.B. and L.M., by the Deutsche Forschungsgemeinschaft (Bu956/6 to T.B. and T.H.), and by University "Roma Tre" CLAR 2005 Grant to P.A. M.B. is grateful to CIMAINA (University of Milano) and to Fondazione CARIPLO (Milano, Italy) for continuous support. S.D. is a postdoctoral fellow of the Fund for Scientific Research-Flanders (FWO).

[‡] The coordinates and structure factors have been deposited as PDB entries 2g3h and r2g3hsf.

* To whom correspondence should be addressed: Department of Biomolecular Sciences and Biotechnology, University of Milano, Via Celoria, 26, I-20133 Milano, Italy. Telephone: +39 02 5031 4893. Fax: +39 02 5031 4895. E-mail: martino.bolognesi@unimi.it.

[§] Universidade Nova de Lisboa.

[||] INMI-IRCCS 'Lazzaro Spallanzani', Roma.

[⊥] University of Antwerp.

[@] Institute of Zoology, Johannes Gutenberg University of Mainz.

[#] Institute of Molecular Genetics, Johannes Gutenberg University of Mainz.

[+] University of Milano.

[1] Abbreviations: Hb, hemoglobin; Mb, myoglobin; trHb, truncated hemoglobin; Dm-glob1, *D. melanogaster* Hb; 6C-Dm-glob1, hexacoordinate Dm-glob1; 5C-Dm-glob1, pentacoordinate Dm-glob1; Dm-glob1$^+$, ferric Dm-glob1; Dm-glob1-CN, cyanide derivative of Dm-glob1$^+$; rms, root-mean-square.

10.1021/bi060462a CCC: $33.50
Published on Web 08/01/2006

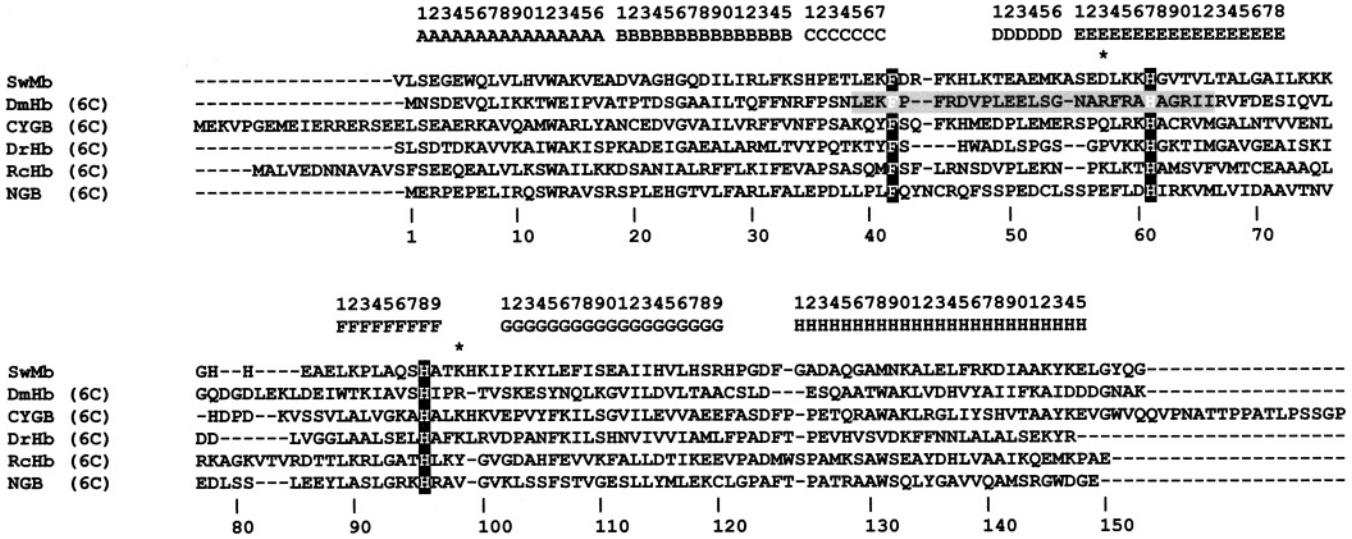

FIGURE 1: Amino acid sequence alignments for Hbs. The primary structures of representative 6C Hbs are aligned, on the basis of available three-dimensional structures, with the reference sequence of sperm whale Mb (SwMb), taken as the reference mammalian globin. DmHb, *D. melanogaster* Hb; CYGB, human cytoglobin; DrHb, *Danio rerio* Hb; RcHb, rice Hb; NGB, human neuroglobin. Amino acid sequences were from http://www.expasy.org/prot/. The topological positions (on top of sequences) refer to the classical globin fold, as defined on sperm whale Mb; the DmHb sequence numbering is reported below the sequences. Residues relevant for the discussion and conserved in the globin fold are highlighted in black. The gray shaded area highlights the protein region affected by conformational changes when endogenous hexacoordination is disrupted by the exogenous ligand. The Arg residues salt-linked to heme propionates are denoted with asterisks.

(i.e., the distal E7 residue) before binding to the heme Fe atom becomes possible. The binding reaction thus displays three steps: (i) removal of the endogenous HisE7 ligand, (ii) formation of a transient reactive heme pentacoordinated (5C) species, and (iii) binding of the external ligand. Heme hexacoordination (6C) is therefore a new mechanism of fine-tuning the binding affinity of exogenous ligands to Hbs (*13*, *15*−*17*). The function of these 6C Hbs is not yet clear, but the involvement in the protection against the consequences of hypoxia by improving oxygen availability (*12*) and/or by detoxification of reactive oxygen or nitrogen species seems likely (*18*−*20*). It has recently been shown that three globin genes (*glob1*, *glob2*, and *glob3*) are present in the genome of *Drosophila melanogaster*, two of which are expressed (*glob1*-Hb1 and *glob2*-Hb2) (*21*−*23*). In situ hybridization and immunohistochemical localization reveal that Hb1 is expressed in the tracheal system and in the fat body of embryonic, larval, and adult flies (*21*, *23*).

Despite the low degree of structural homology to standard globins, the amino acid sequences translated from the *Drosophila* globin gene variants show the major structural determinants of the globin fold, thus hinting at potentially functional Hbs (Figure 1) (*22*, *24*). Moreover, the *Drosophila* globins are significantly similar to the other known insect Hbs (Chironimidae, *G. intestinalis*) (*5*, *6*, *25*). Spectroscopic data show that recombinant Hb1 (Dm-glob1) hosts a 6C heme Fe atom, with His−Fe^{2+}−His axial ligands. Flash photolysis experiments with Dm-glob1 show that O_2 binds through a fast oxygen association process to a transient 5C form of the protein. Nevertheless, the overall O_2 affinity, 0.12 Torr, is lower than expected because of competition between the endogenous ligand (HisE7) and the external ligand (*23*).

In the context of our ongoing studies about the biological role of 6C Hbs and the molecular mechanisms regulating heme−ligand binding and Hb action (*4*, *10*), we report here the three-dimensional structure of Dm-glob1 in its cyano-met form at 1.40 Å resolution. We show that the exogenous ligand displaces the endogenous HisE7 residue, inducing structural rearrangements within the heme distal cavity that are Dm-glob1-specific and affect the main protein backbone in the CD−D−E region and partly the heme location.

EXPERIMENTAL PROCEDURES

Protein Preparation. Recombinant Dm-glob1-O_2 was expressed and purified as previously reported (*4*). The ferric form of Dm-glob1 (Dm-glob1$^+$) was prepared by oxidation of Dm-glob1-O_2 with a 10-fold excess of potassium ferricyanide. After the reaction was allowed to proceed to completion, the protein was purified from ferri/ferrocyanide by desalting over a HiTrap desalting column prepacked with Sephadex G-25 Superfine equilibrated with 1.0×10^{-1} M phosphate buffer (pH 7.0) (*26*).

Kinetic Measurements. The kinetics for binding of cyanide to Dm-glob1$^+$ was followed spectrophotometrically between 350 and 500 nm. Experiments were carried out by mixing Dm-glob1$^+$ (final concentration of $\sim 5.0 \times 10^{-6}$ M) with different amounts of cyanide (i.e., HCN; final concentration of 3.0×10^{-5} to 6.0×10^{-4} M). Kinetics was analyzed within the framework of the minimum reaction mechanism (Scheme 1) (*26*):

Scheme 1

$$\text{6C-Dm-glob1}^+ \xrightarrow{\text{fast}} \text{5C-Dm-glob1}^+$$

$$\text{5C-Dm-glob1}^+ + \text{HCN} \xrightarrow{k_{on}} \text{Dm-glob1-CN} + \text{H}^+$$

in which (i) the rate of dissociation of His(61)E7 from the heme Fe atom is fast in comparison to the first-order rate constant for binding of cyanide to Dm-glob1$^+$ (i.e., k) and (ii) the rate of dissociation of cyanide from Dm-glob1-CN is negligible in comparison to k (see Results and Discussion).

Table 1: Data Collection and Refinement Statistics for Dm-glob1-CN

wavelength (Å)	0.98400
resolution (Å)	35.5−1.40
mosaicity (deg)	0.52
completeness (%)	100.0 (100.0)[a]
R_{merge} (%)	9.4 (21.2)
total no. of reflections	118026
no. of unique reflections	16745
redundancy	3.7 (3.6)
average $I/\sigma(I)$	12.1 (6.3)
statistics and model quality	
no. of protein atoms (non-hydrogen)	1676
no. of water molecules	262
R_{gen}/R_{free} (%)	15.4/18.8
space group	$P2_1$
unit cell dimensions	$a = 43.3$ Å, $b = 33.7$ Å, $c = 56.1$ Å, $\beta = 94.4°$
rms deviation from ideal geometry	
bond lengths (Å)	0.015
bond angles (deg)	1.504
Ramachandran plot (%)[b]	
most favored region	95.6
additional allowed region	4.4
estimated atom positional error (Å)	0.070

[a] Outer shell statistics (1.48−1.40 Å). [b] Data produced using PROCHECK (*54*).

The value of the second-order rate constant for binding of cyanide to Dm-glob1$^+$ (i.e., k_{on}) has been determined from the linear dependence of k on the cyanide concentration (i.e., [HCN]), under pseudo-first-order conditions (i.e., [HCN] > [Dm-glob1]), according to eqs 1 and 2 (*26*):

$$[\text{Dm-glob1-CN}]_t = [\text{Dm-glob1}^+]_i \times e^{-kt} \quad (1)$$

$$k = k_{on}[\text{HCN}] \quad (2)$$

Crystal Structure Analysis. A stock solution of Dm-glob1$^+$ was concentrated to a final protein concentration of 72 mg/mL, previously proven to be suitable for crystallization purposes (*4*). Dm-glob1-CN crystals were grown by vapor diffusion against 34% (w/v) PEG 4000, 200 mM $MgCl_2$, and 50 mM CAPS (pH 10.5); 5.0 mM KCN was systematically added to the protein droplets before crystallization. Under these conditions, well-shaped prismatic crystals of ~300 μm × ~50 μm × ~50 μm grew in 1 week. For X-ray data collection purposes, the crystals were transferred to the same buffer medium used for crystallization, but containing 40% (w/v) PEG 4000 for cryoprotection. X-ray diffraction data, to a maximum resolution of 1.40 Å, were collected at ESRF (Grenoble, France), on beamline ID23-1, using one frozen crystal (100 K), at a λ of 0.9840 Å (Table 1). The collected data were reduced and scaled using MOSFLM and SCALA, respectively (*27*, *28*). The structure was determined by molecular replacement using the structure of 6C-Dm-glob1$^+$ as a search model (PDB entry 2bk9), using MOLREP (*29*). The electron density map was then improved using ARP/wARP (*30*), based on the atomic coordinates of the molecular replacement solution for calculating initial phases. The best map was subsequently autotraced by ARP/wARP (R_{gen} = 29.5%; R_{free} = 29.7%). The initial model [lacking the Leu(76)E22−Asp(79)EF3 loop] was subsequently refined using REFMAC (*31*). The calculated electron density map allowed manual building of the missing loop using O (*32*); further refinement cycles yielded R_{gen} and R_{free} values of 17.9 and 20.3%, respectively. Finally, individual anisotropic atomic *B*-factors were refined using REFMAC (*31*) (R_{gen} = 16.1%; R_{free} = 19.6%); in the last refinement cycle, hydrogen atoms were added in their riding positions (R_{gen} = 15.4%; R_{free} = 18.8%). The final model contains 153 residues, 262 water molecules, one octahedral aquo−Mg complex, two chloride anions, and one cyanide anion (Table 1). Atomic coordinates and structure factors for Dm-glob1-CN have been deposited in the Protein Data Bank, as entries 2g3h and r2g3hsf, respectively (*33*).

RESULTS

Kinetics of Binding of Cyanide to Ferric Dm-glob1. The absorption spectrum of Dm-glob1$^+$ in the Soret region (Figure 2A) is reminiscent of that reported for the imidazole derivative of ferric hemoproteins (*34*, *35*). Such a finding is in keeping with the bis-histidyl coordination state of the heme Fe atom of Dm-glob1$^+$ (*4*). Conversely, the absorption spectrum of Dm-glob1-CN (Figure 2A) is closely similar to that reported for the cyanide derivative of ferric hemoproteins (*26*, *34*).

The time course for binding of cyanide to Dm-glob1$^+$ conforms to a single-exponential decay and is independent of the observation wavelength, at a fixed cyanide concentration (Figure 2B). Values of k for binding of cyanide to Dm-glob1$^+$ are linearly dependent on HCN concentration over the whole ligand concentration range that was explored (i.e., between 3.0×10^{-5} and 6.0×10^{-4} M) (Figure 2C), and with a y intercept at 0, the slope corresponding to k_{on} (see Scheme 1 and eq 2) equals $(1.8 \pm 0.2) \times 10^2$ M^{-1} s^{-1} at pH 7.0 and 20.0 °C (Table 2). Therefore, the value of the first-order rate constant for cyanide dissociation (i.e., k_{off}) is $<1 \times 10^{-3}$ s^{-1}, and the value of the association equilibrium constant K ($=k_{on}/k_{off}$) is $>2 \times 10^5$ M^{-1}. Moreover, the linear dependence of k on HCN concentration (Figure 2C) indicates that the rate constant for dissociation of His(61)E7 from the heme Fe atom of Dm-glob1$^+$ (i.e., fast; see Scheme 1) must exceed by at least 2 orders of magnitude the value of k (0.12 s^{-1}) obtained at the highest HCN concentration that was investigated (6.0×10^{-4} M), i.e., ≥ 12 s^{-1} (Figure 2C); otherwise, a hyperbolic plot would be observed (*36*, *37*).

Values of k_{on} for binding of cyanide to ferric prototypical monomeric hemoproteins are essentially unaffected by the heme Fe geometry (Table 2). In fact, *Aplysia limacina* Mb and *Mycobacterium tuberculosis* trHbN are 5C systems (*37*−*42*), horse Mb and sperm whale Mb bind a loose water molecule at the sixth coordination position of the heme Fe(III) atom (*38*, *41*, *43*−*45*), and Dm-glob1 and *Chlamydomonas eugametos* trHbN are 6C systems (*4*, *37*, *46*), around neutrality. Note that the reactivity of cyanide toward ferric hemoproteins has been postulated to be influenced mainly by the presence in the heme pocket of the proton acceptor group(s), held to assist the deprotonation of the incoming ligand (i.e., HCN). This interpretation is in agreement with (i) the very slow kinetics of binding of cyanide to *Glycera dibranchiata* monomeric Hb (component C) (see Table 2), which lacks both the heme Fe(III)-bound water molecule and the residue(s) catalyzing proton exchange, and (ii) the effect of changes in the polarity of the heme distal pocket of human Mb, pig Mb, and sperm whale Mb detected by site-directed mutagenesis (*26*, *38*, *47*, *48*).

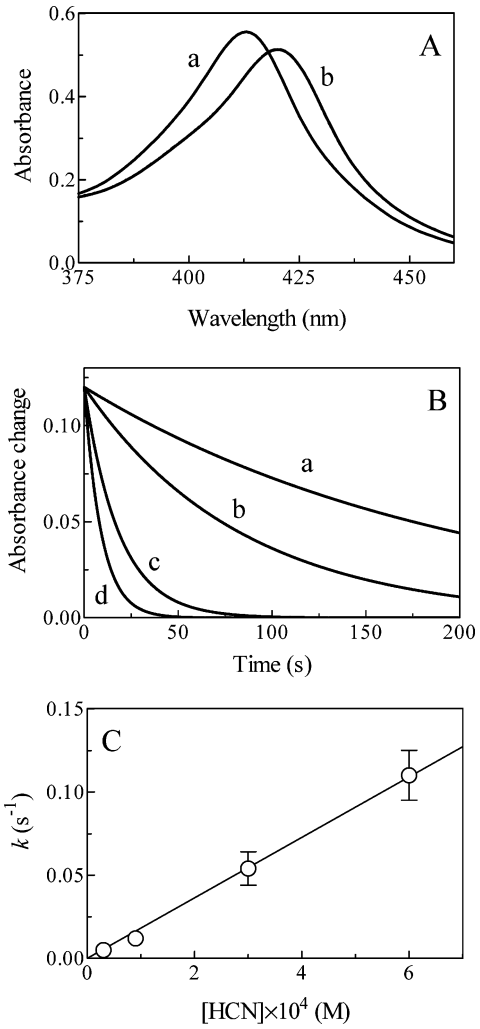

FIGURE 2: Binding of cyanide to ferric Dm-glob1. (A) Absorption spectra in the Soret region of the bis-histidyl (a) and cyanide (b) derivatives of Dm-glob1$^+$, where [Dm-glob1$^+$] $\sim 5.0 \times 10^{-6}$ M and [HCN] $= 1.0 \times 10^{-3}$ M. (B) Time course of binding of cyanide to Dm-glob1$^+$, where [Dm-glob1$^+$] $\sim 5.0 \times 10^{-6}$ M, [HCN] $= 3.0 \times 10^{-5}$ (trace a), 9.0×10^{-5} (trace b), 3.0×10^{-4} (trace c), and 6.0×10^{-4} M (trace d), and $\lambda = 412$ nm. The analysis of the time course according to eq 1 (*26*) allowed us to determine the following values: $k = 0.0050$ (trace a), 0.012 (trace b), 0.054 (trace c), and 0.11 s^{-1} (trace d). (C) Dependence of the pseudo-first-order rate constant for binding of cyanide to Dm-glob1$^+$ (i.e., k) on the HCN concentration. The solid line was calculated according to eq 2 (*26*) where $k_{on} = (1.8 \pm 0.2) \times 10^2$ M^{-1} s^{-1} (Table 1). All data were obtained at pH 7.0 (1.0×10^{-1} M phosphate buffer) and 20.0 °C. For further details, see the text.

The very slow biphasic kinetics of binding of cyanide to ferric 6C human neuroglobin (NGB; see Table 2) does not appear to be limited by dissociation of the heme distal HisE7 residue but reflects the presence of two distinct conformations of the protein (open and closed) in which the heme pocket is more or less accessible to exogenous ligands (e.g., CO) (see ref *20*).

Crystal Structure of Ferric Dm-glob1-CN. Crystallization of Dm-glob1-CN under conditions matching those of the orthorhombic crystals of 6C-Dm-glob1$^+$ yielded a new crystal form (monoclinic space group $P2_1$, $a = 43.31$ Å, $b = 33.71$ Å, $c = 56.06$ Å, $\beta = 94.4°$, one molecule per asymmetric unit). The three-dimensional structure of Dm-glob1-CN was determined through molecular replacement techniques, using the 6C-Dm-glob1$^+$ parent structure as the search model (*4*). Analysis of the crystal packing contacts, as previously shown for 6C-Dm-glob1$^+$, indicates that in this crystal form the protein is monomeric, in agreement with solution gel filtration results (*4*, *22*). Inspection of electron density maps, throughout the refinement cycles, allowed us to identify the cyanide molecule bound to the heme Fe(III) atom, on the heme distal site. Furthermore, structural remodeling of the protein backbone (relative to the globin fold of 6C-Dm-glob1$^+$) was required in the C−CD−D region and in the N-terminal segment of the E helix. Refinement of the Dm-glob1-CN crystal structure, including anisotropic *B*-factor refinement and fixed H atoms, converged to a R_{gen} value of 15.4% and an R_{free} of 18.8% at 1.40 Å resolution (see Table 1).

Table 2: Values of the Second-Order Rate Constant for Binding of Cyanide to Monomeric Hemoproteins Related to the Coordination State of the Ferric Heme Fe Atom

hemoprotein	k_{on} (M^{-1} s^{-1})	Fe coordination	sixth Fe ligand
A. limacina Mb[a]	2.0×10^2	pentacoordinate	−
M. tuberculosis trHbN[b]	3.8×10^2	pentacoordinate	−
G. dibranchiata Hb[c]	4.9×10^{-1}	pentacoordinate	−
horse heart Mb[d]	1.7×10^2	hexacoordinate	water molecule
sperm whale Mb[a]	1.4×10^2	hexacoordinate	water molecule
C. eugametos trHbN[b]	4.6×10^2	hexacoordinate	TyrB10
D. melanogaster glob1[e]	1.8×10^2	hexacoordinate	HisE7
human NGB (fast phase)[f]	1.7	hexacoordinate	HisE7
human NGB (slow phase)[f]	3.7×10^{-1}	hexacoordinate	HisE7

[a] At pH 7.0 and 20.0 °C. From ref *55*. [b] At pH 7.0 and 20.0 °C. From ref *26*. [c] Monomeric Hb, component C. At pH 7.0 and 20.0 °C. From ref *48*. [d] At pH 7.0 and 22.0 °C. From ref *34*. [e] At pH 7.0 and 20.0 °C. From this study. [f] At pH 7.2 and 20.0 °C. From ref *20*.

To recognize reliably the protein structural changes induced by ligand binding, the conformationally invariant part of the Dm-glob1 molecule was identified before least-squares superposition of 6C-Dm-glob1$^+$ and Dm-glob1-CN structures was performed. To this aim, ESCET (*49*) was used, considering that a reliable estimate of the Dm-glob1 structurally invariant part is granted by the high resolution of the two crystal structures considered (1.20 and 1.40 Å, respectively). According to the ESCET approach, the regions of Dm-glob1 that are structurally unperturbed in the two protein forms that were compared were the Met(1)−Asn(38)C4 and Ile(66)E12−Asn(151) segments. A structural overlay of 6C-Dm-glob1$^+$ and Dm-glob1-CN was then calculated using only the conformationally invariant parts of the protein (126 Cα pairs, rms deviation of 0.44 Å). After superposition of the two structures, the largest backbone deviations were located in the C−CD−D region and in the N-terminal zone of the E helix [the Leu(39)C5−Ile(65)E11 segment], with a maximum deviation of 2.79 Å at Ala(60)E6 (Figure 3A).

The structural overlay of 6C-Dm-glob1$^+$ and Dm-glob1-CN shows unambiguously that upon cyanide binding the heme becomes slightly more buried in the protein crevice, with a shift of 0.78 Å along the $\alpha-\gamma$ meso axis direction, while the porphyrin plane is rotated by $\sim 10°$ around the $\beta-\delta$ meso axis. At the same time, rearrangements contained within the heme result in a rms deviation of 0.23 Å between the porphyrin rings of 6C-Dm-glob1$^+$ and Dm-glob1-CN (not considering the propionate groups). Although contained, the observed overall relocation of the heme group is coupled to conformational readjustments of hydrophobic residues in the heme crevice [Leu(28)B10, Phe(42)CD1, Ile(65)E11, Phe-

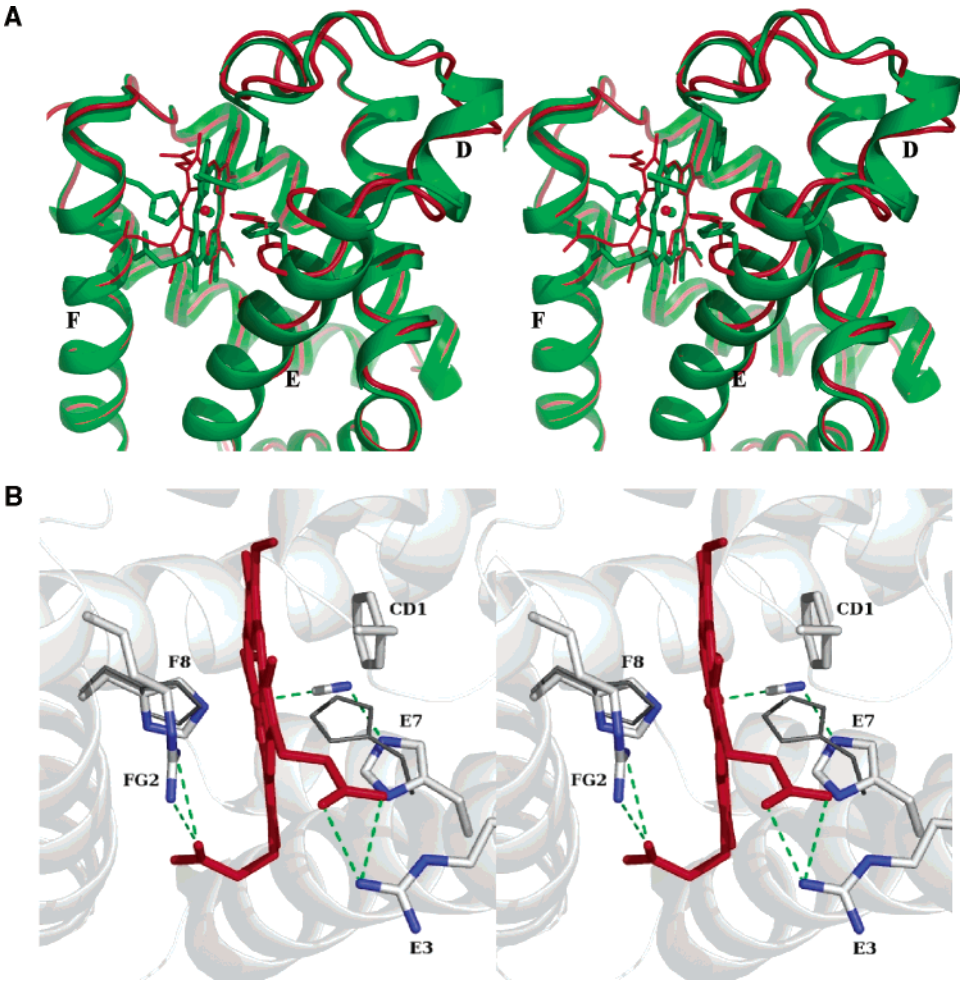

FIGURE 3: Structural details of binding of cyanide to ferric Dm-glob1. (A) Stereoview of the backbone and heme shifts occurring in the 6C-Dm-glob1$^+$ → Dm-glob1-CN transition; 6C-Dm-glob1$^+$ and Dm-glob1-CN structures are colored red and green, respectively. Parts of distal helices B, C, and E, and of the CD region, are displayed together with part of the proximal F helix and the heme. (B) Stereoview showing details of the heme distal site cavity structure of Dm-glob1-CN. Residues Phe(42)CD1, His(61)E7, and His(96)F8, the heme, and the cyanide ligand are shown and labeled, together with residues Arg(57)E3 and Arg(99)FG2 stabilizing the heme through salt bridges. The hydrogen bonds are shown as dashed lines: the location of the distal and proximal heme ligands [His(61)E7 and His(96)F8, respectively], as observed in the crystal structure of 6C-Dm-glob1$^+$, are displayed using thin gray lines [drawn with Pymol (*56*)]. For further details, see the text.

(69)E15, and Trp(89)F1] that provide van der Waals contacts to the porphyrin ring, or fill the distal cavity, in both 6C-Dm-glob1$^+$ and the cyano-met form.

Since 6C-Dm-glob1$^+$ and Dm-glob1-CN crystals belong to different space groups, different inter- and intramolecular interactions were observed. In particular, Arg(99)FG2, which in 6C-Dm-glob1$^+$ is hydrogen-bonded to heme propionate D, is salt-linked to propionate A in Dm-glob1-CN. Conversely, Arg(57)E3, which in 6C-Dm-glob1$^+$ was interacting with a symmetry equivalent molecule, in Dm-glob1-CN is salt-linked (and hydrogen-bonded) to propionate D, within the same protein molecule. Thus, both Arg(57)E3 and Arg(99)FG2 stabilize the heme in its slightly altered location following cyanide binding.

On the proximal side of the heme, the His(96)F8 coordination bond to the heme Fe atom (2.05 Å) is orthogonal to the porphyrin plane; the proximal HisF8 imidazole ring is tilted by ~12° relative to 6C-Dm-glob1$^+$ as a result of the heme sliding movement mentioned above, while maintaining an essentially unaltered His(96)F8 Cα position. On the heme distal side, the cyanide ligand provides a coordination bond of 2.03 Å to the heme Fe atom, being almost orthogonal (86°) to the heme plane; the angle defined by atoms $NE2_{HisF8}$, Fe, and $C1_{cyanide}$ (the Fe axial coordination bonds) is 176°. Remarkably, the heme Fe axial ligands display coordination bonds that closely match those established by the Fe atom and the heme pyrrole N atoms (average of 1.98 Å). Thus, the observation of a rather regular heme Fe coordination sphere, and the orientation of the cyanide ligand (orthogonal to the heme), suggest that no significant reduction of the heme Fe atom has occurred during X-ray data collection. Conversely, (partial) reduction of the heme Fe atom has been reported for several homologous Hbs or Mbs, resulting in sizable elongation of the Fe−CN axial coordination bond, and in a bent orientation of the ligand (*50*).

As discussed above, binding of cyanide to the heme distal site of 6C-Dm-glob1$^+$ causes the replacement of the endogenous His(61)E7 ligand. From the structural viewpoint, such a process is essentially the result of a rigid-body protein backbone shift rather than of His(61)E7 side chain conformational readjustments. In particular, following cyanide binding, the N-terminal half of the E helix is shifted away from the heme, roughly pivoting around residue Ile(66)E12, resulting in a shift of 2.4 Å at the Cα atom of His(61)E7 of

Dm-glob1-CN relative to 6C-Dm-glob1$^+$. Remarkably, the side chain of His(61)E7 follows the rigid-body shift of part of the E helix, displaying a 12° rotation around the Cβ−Cγ bond, and a 180° rotation of the imidazole ring (by rotation around the Cγ−Cδ bond), thus presenting the side chain NE2 atom to the heme-bound ligand (Figure 3B). As a result, the imidazole ring of His(61)E7, directly coordinated to the heme Fe atom in 6C-Dm-glob1$^+$, moves 2.7 Å away from the heme, but it is not swung out of the heme pocket, likely because of a strong hydrogen bond linking the His(61)E7 NE2 atom to the N atom of the cyanide ligand (2.68 Å). Qualitatively comparable shifts, resulting from the rigid-body backbone shift, affect all distal residues that make up the CD−D and first part of the E helix regions. The notable exception in this context is residue Ile(65)E11, whose backbone is shifted as well, but whose side chain conformation varies substantially (~90° rotation around the Cα−Cβ bond) in relation to altered contacts with the porphyrin ring. Considering the heme shifts described above for the two Dm-glob1 forms, it appears that contacts exerted by His(61)E7 on the porphyrin ring in 6C-Dm-glob1$^+$ are partly released in Dm-glob1-CN, resulting in a reduced level of doming of the heme, responsible, together with the new heme location, for the altered contacts with Ile(65)E11. As a whole, the structural rearrangements observed in Dm-glob1-CN increase the volume of the heme distal cavity by ~35 Å^3.

Finally, from inspection of the whole protein structures, it can be concluded that the conformational changes characterizing the transition between 6C-Dm-glob1$^+$ and Dm-glob1-CN are located in the extended distal region described above. A minor conformational change (largest shift of 1.6 Å) affecting residues Gly(77) and Gln(78), in the EF hinge region of Dm-glob1-CN, is likely related to the absence of a CAPS buffer molecule bound to a nearby protein surface cavity in the orthorhombic crystals of 6C-Dm-glob1$^+$ (*4*). Additionally, inspection of the Dm-glob1-CN structure shows that, despite the conformational rearrangements reported above, upon cyanide binding the small three-protein matrix cavities recognized in 6C-Dm-glob1$^+$ are unperturbed in their size and locations within the protein matrix.

DISCUSSION

The structural data presented here indicate that the transition from 6C-Dm-glob1$^+$ to Dm-glob1-CN is characterized by two distinct orders of phenomena. On one hand, release of endogenous hexacoordination, a prerequisite for cyanide binding, and heme Fe atom exogenous ligation allow a contained but sizable repositioning of the heme in its crevice. Such repositioning results from heme shifts, from heme rotation, and, to a lesser extent, from the transition from a modestly domed porphyrin to a more planar conformation. Comparison of the 6C-Dm-glob1$^+$ and Dm-glob1-CN structures suggests that contacts with His(61)E7 may be the primary cause of heme doming in 6C-Dm-glob1$^+$. The second series of conformational events concern the distal part of the protein backbone that make up the CD−D portion and part of the E helix region. Here the observed global backbone shift, away from the heme, may be triggered by loss of the His(61)E7 coordination bond to the heme Fe atom, which would allow Dm-glob1-CN to relax into a backbone conformation more closely related (in the CD−D−E regions) to that of the cyanide derivative of ferric sperm whale Mb (*50*). Such an observation would suggest that in Dm-glob1 the endogenous 6C state is a strained one [His(61)E7 closing on the heme] that is relaxed when the His(61)E7−heme Fe coordination bond is severed. This hypothesis has two implications. On one hand, the His(61)E7−heme Fe coordination bond itself would be strained and thus less stable than the proximal His(96)F8−heme Fe bond, reflecting the protein trend toward an open pentacoordinate (i.e., 5C) state. On the other hand, facilitated rupture of the His(61)E7−heme Fe coordination bond may be a structural property coded in hexacoordinate (i.e., 6C) Hbs, if affinity for the exogenosus ligand(s) (e.g., O_2) has to be kept within a physiologically relevant range (*51*). The observation that kinetics of binding of cyanide to ferric 6C-Dm-glob1$^+$ follows the binding pattern observed for homologous hemoproteins (not displaying hexacoordination in their ligand-free states) suggests that the rupture of the endogenous heme Fe−His(61)E7 coordination bond is a process readily achieved in 6C-Dm-glob1, in keeping with such structural and functional considerations.

Only two structural comparisons with 6C Hbs, for which both the endogenously and exogenously liganded protein structures are known, can be thought to validate (at least on a qualitative basis) the hypotheses given above. As a first case, we consider human cytoglobin, whose crystal structure displays both the endogenous 6C form and a 5C species, although the latter is devoid of the heme distal ligand (in the ferric form) (*15*). In this case, the rupture of the HisE7−heme Fe coordination bond is mirrored by conformational transitions in the CD−E regions quite comparable to those reported here for Dm-glob1-CN. The cytoglobin case would then support a mechanism for the transition of the heme distal cavity from endogenous to exogenous ligation in which the conformational flexibility of the CD−D region and part of the E helix regions is instrumental in assisting in the removal of the distal HisE7 residue from the heme sixth coordination site.

Second, the case of mouse neuroglobin can be considered (*14*, *52*). Upon CO binding, mouse neuroglobin is characterized by a remarkable sliding of the heme group in the direction of the EF hinge, which leaves mostly unperturbed the locations of HisE7 and of the supporting E helix (as well as of the CD−D region). The overall protein response to the transition toward ligation of the exogenous CO ligand, including heme shifts, thus, takes place in directions which differ from those observed for Dm-glob1. In particular, the protein backbone conformational readjustments in the distal region of the heme crevice are very contained (the Cα displacement at residue HisE7 of the overlayed 6C mouse Ngb and its CO derivative is 0.56 Å, with a shift of 0.7 Å in the HisE7 imidazole ring in the two protein forms), not suggesting the extended rigid-body segmental reshaping of the CD−D−E region seen in Dm-glob1-CN. Conversely, with respect to the need to create room for the exogenous CO ligand in the distal pocket, the heme group is relocated, with a move composed of sliding into the heme crevice, tilting, and increased doming, resulting in a shift of ~1.8 Å at the Fe atom (larger at the rims of the porphyrin ring) in the two protein forms. Such moves have a sizable effect on the proximal HisF8 residue of mouse neuroglobin, whose heme Fe coordinated NE2 atom moves ~1.7 Å upon CO ligation.

The different shifts of the heme, and most notably the conformational transitions accepted by the CD−D (and partly E) regions, are a structural property that differently characterizes carbonylated mouse neuroglobin, Dm-glob1-CN, and 5C (ligand-free) human cytoglobin. Such a property is worth noticing further in light of the conformational disorder observed in the CD−D region of the homologous human 6C neuroglobin (*53*). In fact, human 6C neuroglobin, whose crystal structure displays four independent molecules per asymmetric unit, shows two fully disordered and two fully ordered CD−D regions, in the crystallized molecules. Such an observation, in keeping with the very slow biphasic kinetics of binding of cyanide to ferric 6C human neuroglobin (*20*), might indicate that the distal region is ready to accept conformational transitions depending on the different protein-liganded states.

In agreement with the extensive preceding literature on binding of cyanide to monomeric hemoproteins, the new inclusion of structural and kinetic data on binding of cyanide to Dm-glob1$^+$ (a 6C Hb) confirms that the process is scarcely affected (in the different proteins) by local structural properties defining the ligand diffusion/binding mechanism to the heme distal pocket. Although such an observation is supported by comparison of the ligand association rate constants of Dm-glob1$^+$ with several Mbs or Hbs from widely different sources (see Table 2), it is worth noting that kinetic differences (and stages) are displayed by human neuroglobin, a 6C Hb. This study indicates, in fact, that the complex mechanism of balancing endogenous versus exogenous heme hexacoordination processes in different 6C Hbs may be achieved very differently.

REFERENCES

1. Willmer, P., Stone, G., and Johnston, I. A. (2000) *Environmental Physiology of Animals*, Blackwell Press, Oxford, U.K.
2. Brusca, R. C., and Brusca, G. J. (1990) *Invertebrates*, Sinauer, Sunderland, MA.
3. Weber, R. E., and Vinogradov, S. N. (2001) Nonvertebrate hemoglobins: Functions and molecular adaptations, *Physiol. Rev. 81*, 569−628.
4. de Sanctis, D., Dewilde, S., Vonrhein, C., Pesce, A., Moens, L., Ascenzi, P., Hankeln, T., Burmester, T., Ponassi, M., Nardini, M., and Bolognesi, M. (2005) Bishistidyl heme hexa-coordination, a key structural property in *Drosophila melanogaster* hemoglobin, *J. Biol. Chem. 280*, 27222−9.
5. Dewilde, S., Blaxter, M., Van Hauwaert, M. L., Van Houte, K., Pesce, A., Griffon, N., Kiger, L., Marden, M. C., Vermeire, S., Vanfleteren, J., Esmans, E., and Moens, L. (1998) Structural, functional, and genetic characterization of *Gasterophilus* hemoglobin, *J. Biol. Chem. 273*, 32467−74.
6. Hankeln, T., Amid, C., Weich, B., Niessing, J., and Schmidt, E. R. (1998) Molecular evolution of the globin gene cluster E in two distantly related midges, *Chironomus pallidivittatus* and *C. thummi thummi*, *J. Mol. Evol. 46*, 589−601.
7. Pesce, A., Nardini, M., Dewilde, S., Hoogewijs, D., Ascenzi, P., Moens, L., and Bolognesi, M. (2005) Modulation of oxygen binding to insect hemoglobins: The structure of hemoglobin from the botfly *Gasterophilus intestinalis*, *Protein Sci. 14*, 3057−63.
8. Steigemann, W., and Weber, E. (1979) Structure of erythrocruorin in different ligand states refined at 1.4 Å resolution, *J. Mol. Biol. 127*, 309−38.
9. Hagner-Holler, S., Schoen, A., Erker, W., Marden, J. H., Ruprecht, R., Decker, H., and Burmester, T. (2004) A respiratory hemocyanin from an insect, *Proc. Natl. Acad. Sci. U.S.A. 101*, 871−4.
10. Vinogradov, S. N., Hoogewijs, D., Bailly, X., Arredondo-Peter, R., Guertin, M., Gough, J., Dewilde, S., Moens, L., and Vanfleteren, J. R. (2005) Three globin lineages belonging to two structural classes in genomes from the three kingdoms of life, *Proc. Natl. Acad. Sci. U.S.A. 102*, 11385−9.
11. Wittenberg, J. B., Bolognesi, M., Wittenberg, B. A., and Guertin, M. (2002) Truncated hemoglobins: A new family of hemoglobins widely distributed in bacteria, unicellular eukaryotes, and plants, *J. Biol. Chem. 277*, 871−4.
12. Hankeln, T., Ebner, B., Fuchs, C., Gerlach, F., Haberkamp, M., Laufs, T. L., Roesner, A., Schmidt, M., Weich, B., Wystub, S., Saaler-Reinhardt, S., Reuss, S., Bolognesi, M., Sanctis, D. D., Marden, M. C., Kiger, L., Moens, L., Dewilde, S., Nevo, E., Avivi, A., Weber, R. E., Fago, A., and Burmester, T. (2005) Neuroglobin and cytoglobin in search of their role in the vertebrate globin family, *J. Inorg. Biochem. 99*, 110−9.
13. Pesce, A., Nardini, M., Dewilde, S., Ascenzi, P., Burmester, T., Hankeln, T., Moens, L., and Bolognesi, M. (2002) Human neuroglobin: Crystals and preliminary X-ray diffraction analysis, *Acta Crystallogr. D58*, 1848−50.
14. Vallone, B., Nienhaus, K., Brunori, M., and Nienhaus, G. U. (2004) The structure of murine neuroglobin: Novel pathways for ligand migration and binding, *Proteins 56*, 85−92.
15. de Sanctis, D., Dewilde, S., Pesce, A., Moens, L., Ascenzi, P., Hankeln, T., Burmester, T., and Bolognesi, M. (2004) Crystal structure of cytoglobin: The fourth globin type discovered in man displays heme hexa-coordination, *J. Mol. Biol. 336*, 917−27.
16. Hargrove, M. S., Brucker, E. A., Stec, B., Sarath, G., Arredondo-Peter, R., Klucas, R. V., Olson, J. S., and Phillips, G. N., Jr. (2000) Crystal structure of a nonsymbiotic plant hemoglobin, *Structure 8*, 1005−14.
17. Weber, R. E., and Fago, A. (2004) Functional adaptation and its molecular basis in vertebrate hemoglobins, neuroglobins and cytoglobins, *Respir. Physiol. Neurobiol. 144*, 141−59.
18. Brunori, M., Giuffre, A., Nienhaus, K., Nienhaus, G. U., Maria Scandurra, F., and Vallone, B. (2005) Neuroglobin, nitric oxide, and oxygen: Functional pathways and conformational changes, *Proc. Natl. Acad. Sci. U.S.A. 102*, 8483−8.
19. Fago, A., Hundahl, C., Dewilde, S., Gilany, K., Moens, L., and Weber, R. E. (2004) Allosteric regulation and temperature dependence of oxygen binding in human neuroglobin and cytoglobin. Molecular mechanisms and physiological significance, *J. Biol. Chem. 279*, 44417−26.
20. Herold, S., Fago, A., Weber, R. E., Dewilde, S., and Moens, L. (2004) Reactivity studies of the Fe(III) and Fe(II)NO forms of human neuroglobin reveal a potential role against oxidative stress, *J. Biol. Chem. 279*, 22841−7.
21. Burmester, T., and Hankeln, T. (1999) A globin gene of *Drosophila melanogaster*, *Mol. Biol. Evol. 16*, 1809−11.
22. Burmester, T., Storf, J., Hasenjager, A., Klawitter, S., and Hankeln, T. (2006) The hemoglobin genes of *Drosophila*, *FEBS Lett. 273*, 468−80.
23. Hankeln, T., Jaenicke, V., Kiger, L., Dewilde, S., Ungerechts, G., Schmidt, M., Urban, J., Marden, M. C., Moens, L., and Burmester, T. (2002) Characterization of *Drosophila* hemoglobin. Evidence for hemoglobin-mediated respiration in insects, *J. Biol. Chem. 277*, 29012−7.
24. Bashford, D., Chothia, C., and Lesk, A. M. (1987) Determinants of a protein fold. Unique features of the globin amino acid sequences, *J. Mol. Biol. 196*, 199−216.
25. Fukuda, M., Takagi, T., and Shikama, K. (1993) Polymorphic hemoglobin from a midge larva (*Tokunagayusurika akamusi*) can be divided into two different types, *Biochim. Biophys. Acta 1157*, 185−91.
26. Milani, M., Ouellet, Y., Ouellet, H., Guertin, M., Boffi, A., Antonini, G., Bocedi, A., Mattu, M., Bolognesi, M., and Ascenzi, P. (2004) Cyanide binding to truncated hemoglobins: A crystallographic and kinetic study, *Biochemistry 43*, 5213−21.
27. Leslie, A. G. (2006) The integration of macromolecular diffraction data, *Acta Crystallogr. D62*, 48−57.
28. Evans, P. (2006) Scaling and assessment of data quality, *Acta Crystallogr. D62*, 72−82.
29. Vagin, A., and Teplyakov, A. (2000) An approach to multi-copy search in molecular replacement, *Acta Crystallogr. D56* (Part 12), 1622−4.
30. Perrakis, A., Harkiolaki, M., Wilson, K. S., and Lamzin, V. S. (2001) ARP/wARP and molecular replacement, *Acta Crystallogr. D57*, 1445−50.
31. Murshudov, G. N., Vagin, A. A., and Dodson, E. J. (1997) Refinement of macromolecular structures by the maximum-likelihood method, *Acta Crystallogr. D53*, 240−55.

32. Jones, T. A., Zou, J. Y., Cowan, S. W., and Kjeldgaard, M. (1991) Improved methods for building protein models in electron density maps and the location of errors in these models, *Acta Crystallogr. A47* (Part 2), 110−9.
33. Berman, H. M., Westbrook, J., Feng, Z., Gilliland, G., Bhat, T. N., Weissig, H., Shindyalov, I. N., and Bourne, P. E. (2000) The Protein Data Bank, *Nucleic Acids Res. 28*, 235−42.
34. Antonini, E., and Brunori, M. (1971) *Hemoglobin and Myoglobin in their Reactions with Ligands*, North-Holland Publishing Co., Amsterdam.
35. Bolognesi, M., Cannillo, E., Ascenzi, P., Giacometti, G. M., Merli, A., and Brunori, M. (1982) Reactivity of ferric *Aplysia* and sperm whale myoglobins towards imidazole. X-ray and binding study, *J. Mol. Biol. 158*, 305−15.
36. Coletta, M., Ascenzi, P., D'Avino, R., and di Prisco, G. (1996) Proton-linked subunit kinetic heterogeneity for carbon monoxide binding to hemoglobin from *Chelidonichthys kumu*, *J. Biol. Chem. 271*, 29859−64.
37. Couture, M., Das, T. K., Lee, H. C., Peisach, J., Rousseau, D. L., Wittenberg, B. A., Wittenberg, J. B., and Guertin, M. (1999) *Chlamydomonas* chloroplast ferrous hemoglobin. Heme pocket structure and reactions with ligands, *J. Biol. Chem. 274*, 6898−910.
38. Bolognesi, M., Bordo, D., Rizzi, M., Tarricone, C., and Ascenzi, P. (1997) Nonvertebrate hemoglobins: Structural bases for reactivity, *Prog. Biophys. Mol. Biol. 68*, 29−68.
39. Bolognesi, M., Onesti, S., Gatti, G., Coda, A., Ascenzi, P., and Brunori, M. (1989) *Aplysia limacina* myoglobin. Crystallographic analysis at 1.6 Å resolution, *J. Mol. Biol. 205*, 529−44.
40. Conti, E., Moser, C., Rizzi, M., Mattevi, A., Lionetti, C., Coda, A., Ascenzi, P., Brunori, M., and Bolognesi, M. (1993) X-ray crystal structure of ferric *Aplysia limacina* myoglobin in different liganded states, *J. Mol. Biol. 233*, 498−508.
41. Giacometti, G. M., Ascenzi, P., Brunori, M., Rigatti, G., Giacometti, G., and Bolognesi, M. (1981) Absence of water at the sixth co-ordination site in ferric *Aplysia* myoglobin, *J. Mol. Biol. 151*, 315−9.
42. Mukai, M., Savard, P. Y., Ouellet, H., Guertin, M., and Yeh, S. R. (2002) Unique ligand-protein interactions in a new truncated hemoglobin from *Mycobacterium tuberculosis*, *Biochemistry 41*, 3897−905.
43. Aime, S., Fasano, M., Paoletti, S., Arnelli, A., and Ascenzi, P. (1995) NMR relaxometric investigation on human methemoglobin and fluoromethemoglobin. An improved quantitative in vitro assay of human methemoglobin, *Magn. Reson. Med. 33*, 827−31.
44. Perutz, M. F. (1979) Regulation of oxygen affinity of hemoglobin: Influence of structure of the globin on the heme iron, *Annu. Rev. Biochem. 48*, 327−86.
45. Takano, T. (1977) Structure of myoglobin refined at 2.0 Å resolution. I. Crystallographic refinement of metmyoglobin from sperm whale, *J. Mol. Biol. 110*, 537−68.
46. Couture, M., and Guertin, M. (1996) Purification and spectroscopic characterization of a recombinant chloroplastic hemoglobin from the green unicellular alga *Chlamydomonas eugametos*, *Eur. J. Biochem. 242*, 779−87.
47. Brancaccio, A., Cutruzzola, F., Allocatelli, C. T., Brunori, M., Smerdon, S. J., Wilkinson, A. J., Dou, Y., Keenan, D., Ikeda-Saito, M., Brantley, R. E., Jr., and Olson, J. S. (1994) Structural factors governing azide and cyanide binding to mammalian metmyoglobins, *J. Biol. Chem. 269*, 13843−53.
48. Mintorovitch, J., van Pelt, D., and Satterlee, J. D. (1989) Kinetic study of the slow cyanide binding to *Glycera dibranchiata* monomer hemoglobin components III and IV, *Biochemistry 28*, 6099−104.
49. Schneider, T. R. (2002) A genetic algorithm for the identification of conformationally invariant regions in protein molecules, *Acta Crystallogr. D58*, 195−208.
50. Bolognesi, M., Rosano, C., Losso, R., Borassi, A., Rizzi, M., Wittenberg, J. B., Boffi, A., and Ascenzi, P. (1999) Cyanide binding to *Lucina pectinata* hemoglobin I and to sperm whale myoglobin: An X-ray crystallographic study, *Biophys. J. 77*, 1093−9.
51. de Sanctis, D., Pesce, A., Nardini, M., Bolognesi, M., Bocedi, A., and Ascenzi, P. (2004) Structure−function relationships in the growing hexa-coordinate hemoglobin sub-family, *IUBMB Life 56*, 643−51.
52. Vallone, B., Nienhaus, K., Matthes, A., Brunori, M., and Nienhaus, G. U. (2004) The structure of carbonmonoxy neuroglobin reveals a heme-sliding mechanism for control of ligand affinity, *Proc. Natl. Acad. Sci. U.S.A. 101*, 17351−6.
53. Pesce, A., Dewilde, S., Nardini, M., Moens, L., Ascenzi, P., Hankeln, T., Burmester, T., and Bolognesi, M. (2003) Human brain neuroglobin structure reveals a distinct mode of controlling oxygen affinity, *Structure 11*, 1087−95.
54. Laskowski, R. A., MacArthur, M. W., Moss, D. S., and Thornton, J. M. (1993) PROCHECK: A program to check the stereochemical quality of protein structure, *J. Appl. Crystallogr. 26*, 283−91.
55. Nardini, M., Tarricone, C., Rizzi, M., Lania, A., Desideri, A., De Sanctis, G., Coletta, M., Petruzzelli, R., Ascenzi, P., Coda, A., and Bolognesi, M. (1995) Reptile heme protein structure: X-ray crystallographic study of the aquo-met and cyano-met derivatives of the loggerhead sea turtle (*Caretta caretta*) myoglobin at 2.0 Å resolution, *J. Mol. Biol. 247*, 459−65.
56. DeLano, W. L. (2002) *The PyMOL Molecular Graphics System*, DeLano Scientific LLC, San Carlos, CA.

BI060462A